2024

IMPACTS OF SEAFLOOR CHARACTERISTICS ON SOUND PROPAGATION IN A SEAMOUNT ENVIRONMENT

Brendan King
University of Rhode Island, brendan.king2000@gmail.com

IMPACTS OF SEAFLOOR CHARACTERISTICS ON SOUND PROPAGATION IN A SEAMOUNT ENVIRONMENT

BY

BRENDAN KING

A THESIS SUBMITTED IN PARTIAL FULFILLMENT OF

THE

REQUIREMENTS FOR THE DEGREE OF

MASTER OF SCIENCE

IN

OCEAN ENGINEERING

UNIVERSITY OF RHODE ISLAND

2024

MASTER OF SCIENCE IN OCEAN ENGINEERING DEGREE THESIS

OF

BRENDAN KING

APPROVED:

Thesis Committee

Major Professor James H. Miller

Gopu R. Potty

Brice Loose

Brenton DeBoef

DEAN OF THE GRADUATE SCHOOL

UNIVERSITY OF RHODE ISLAND

2024

Abstract

Two modelling programs were used to perform acoustic modeling for the New England Seamount Chain, both around the Atlantis II seamount and the caldera located southeast of Atlantis II. These programs were used for modeling NESMA (New England Seamount Acoustics Experiment) experiments in 2023 and 2024. Varying sound speeds and complex bathymetry within this ocean environment were used in the modelling to see any effects on acoustic propagation. For the Atlantis II seamount scenario, the results of the two models showed some slightly faster arrival times with the warmer water sound speed profiles, as well as showing multiple arrivals with varying interaction between the surface and bottom. Data analysis performed with acoustic data collected in NESMA 2023 showed these multiple sets of arrivals, some complicated by possible scattering and limited accuracy of the propagation models. The model results for the upcoming NESMA 2024 experiment provide insight into the acoustic propagation in the ocean environment around the caldera.

Acknowledgements

Thank you to all the members of my thesis committee. My major professor, Dr. James Miller, for all the guidance, assistance, and advice over the course of my degree. Dr. Gopu Potty for constant modeling and data processing help. Dr. Brice Loose for helping show me different perspectives on my work. Dr. David Taggert for carving time out for me without hesitation. And lastly, I'd like to thank my officemates Jade Case and Haley Green for all the support throughout the ups and downs of this project.

Table of Contents

List of Figures

Chapter 1. Background

Throughout the ocean environment there are plenty of areas that bring their own set of unique intricacies, whether that be a complex bathymetry, such as a seamount or canyon, or varying bottom sediments, such as mud, sand, or limestone, all in which can drastically affect and change acoustic propagation. Organizations, such as the Navy, and researchers want to better understand the acoustical effects these intricacies bring, for the purpose of application to ocean acoustic propagation, timing, navigation, communication and remote sensing.

The Office of Naval Research established a program called Task Force Ocean [cite https://www.nre.navy.mil/organization/departments/code-32/partnerships/task-force-ocean] to solidify a partnership between the Navy, academia, and the private sector, as well as dedicate a set of funding for projects and experiments to help advance Navy-relevant ocean science. Within this new program, the New England Seamount Acoustics Experiment (NESMA) was created with a goal to better understand acoustic propagation in complicated environments with oceanographic and bathymetric features (Navy, 2023). Organizations such as the University of Rhode Island, Woods Hole Oceanographic Institution, Scripps Institution of Oceanography, Naval Postgraduate School, and several academic institutions are combining their efforts to lead the NESMA experiment. The pilot experiment was performed in April-June 2023, with a full experiment planned for the summer months of 2024.

The New England Seamount Chain, including the Atlantis II Seamount, is located roughly 800 km southeast off the coast of Cape Cod, Massachusetts, shown below in Figure 1.

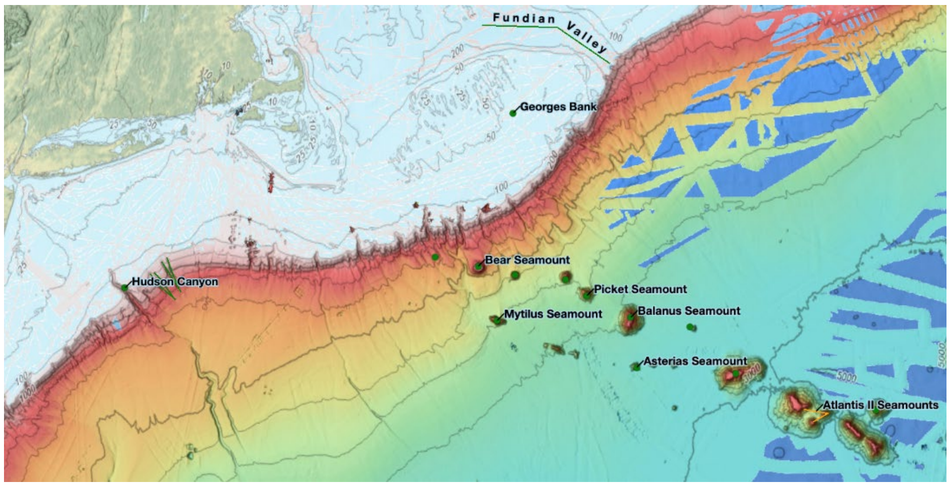

Figure 1. Oceanographic view of the New England Seamount Chain.

Acoustic propagation modeling has been a focus of the acoustics community to utilize as a tool for better understanding the ocean environment around us. Below is a simple schematic showing acoustic propagation in the ocean from a transmitter emitting sound that is received by a hydrophone.

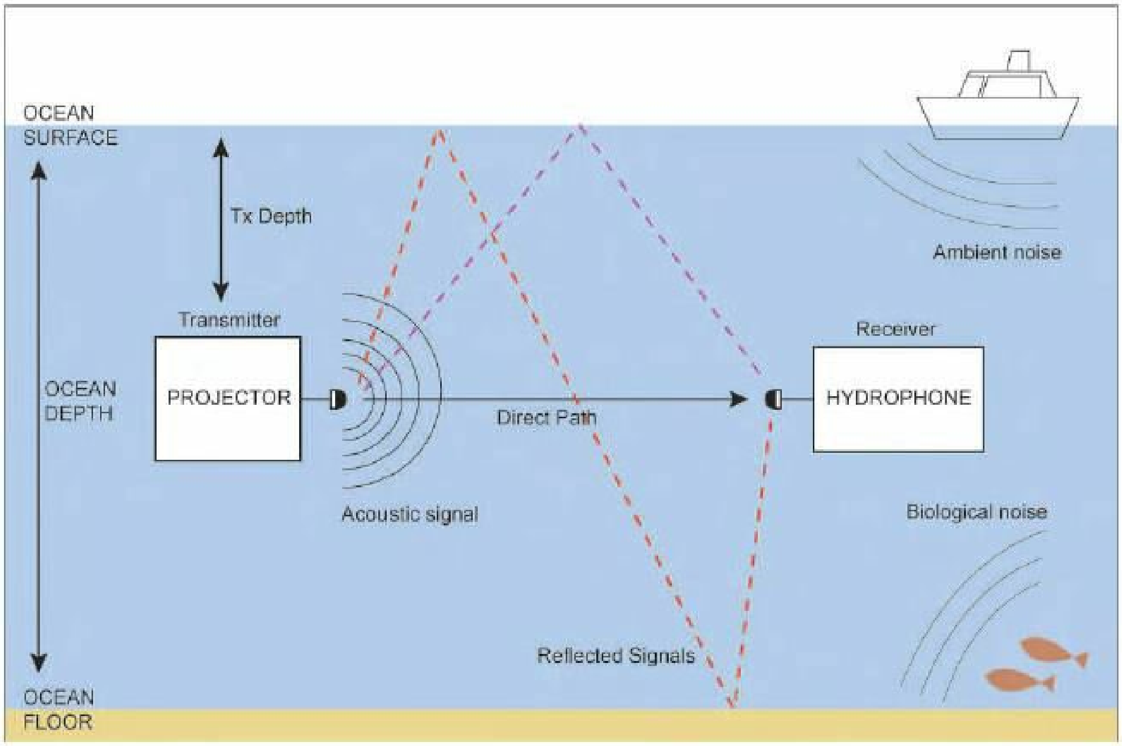

Figure 2. Schematic showing acoustic propagation between a source, transmitter, and a receiver, hydrophone, illustrating possible interactions within the ocean environment.

There are countless factors that can influence the acoustic propagation of an ocean environment, including seafloor properties, bathymetry, varying water temperature, wildlife, surface interaction, etc. Combining the use of these acoustic modeling programs and learning to increase the accuracy and reliability of the models generated from them will allow researchers to continue to analyze any complex ocean environment.

One important goal of the NESMA experiment is to better understand the effect of varying seafloor properties on and around the seamount on acoustic propagation. Measurements of acoustic data enable researchers to more accurately model propagation. This thesis utilizes two modeling programs to represent the acoustic propagation around the seamount: a ray tracing model BELLHOP (Porter M., 2023) and a broadband parabolic equation model MMPE (Tappert F., Smith K. B., 2023). The main purpose of the ray tracing model is to better understand the ray paths sound will take in the analyzed scenarios from the experiment. The MMPE model's main purpose is to better understand and represent the acoustic energy distribution over frequency and time.

Below in Figure 3 is the experimental plan generated by the partnered organizations involved in the planning of the NESMA experiment.

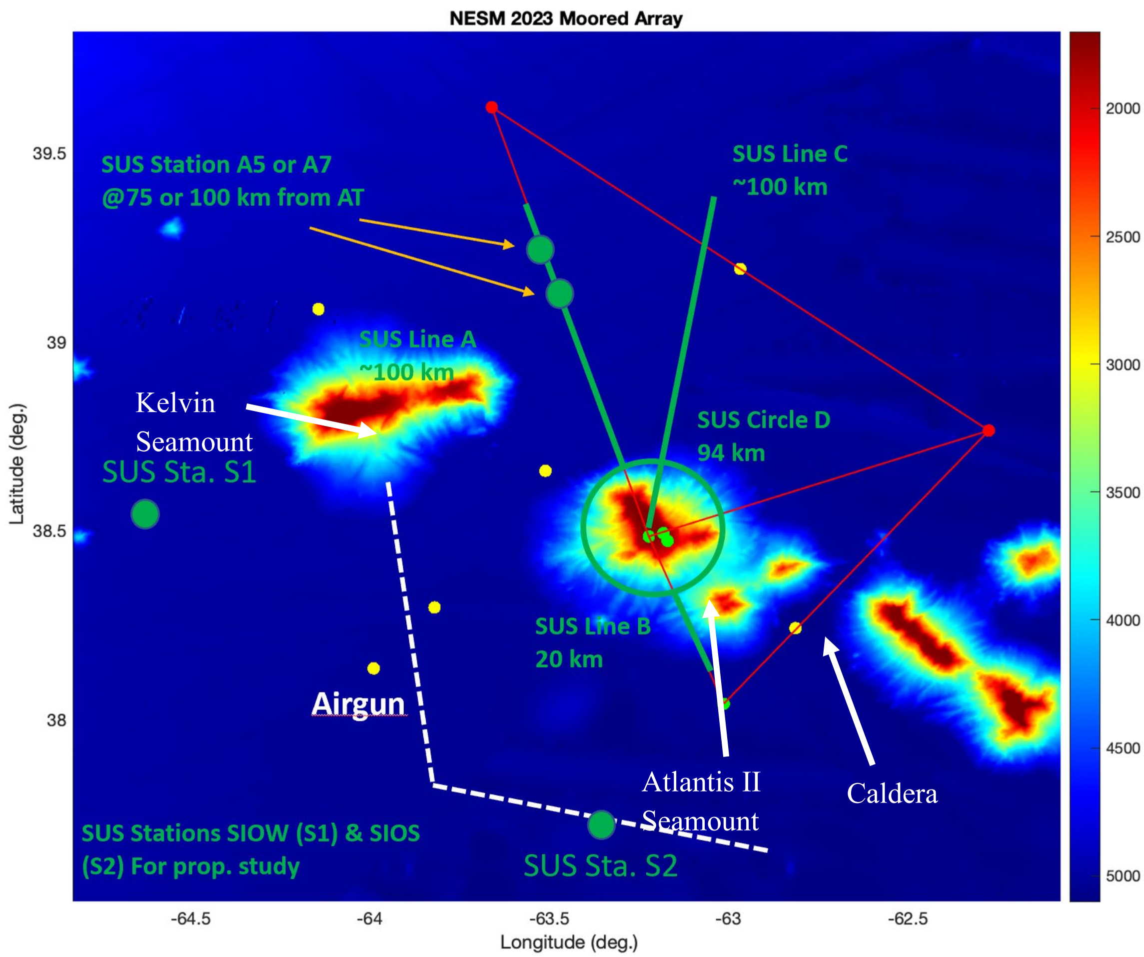

Figure 3. SUS deployment plan for 2023 NESMA Experiment, including sets of SUS lines and circles, and labeled significant geographical locations.

This plan lays out the locations of the various receivers and recorders used to gather acoustic data, as well as the deployment locations of shallow and deep-water broadband SUS charges. The modeling for this thesis narrows its focus onto the short-range acoustic propagation by examining the SUS Circle D, a 15 km radius of SUS charges centered around the center of the Atlantis II seamount. A more detailed view of the SUS Circle D plan is pictured below in Figure 4.

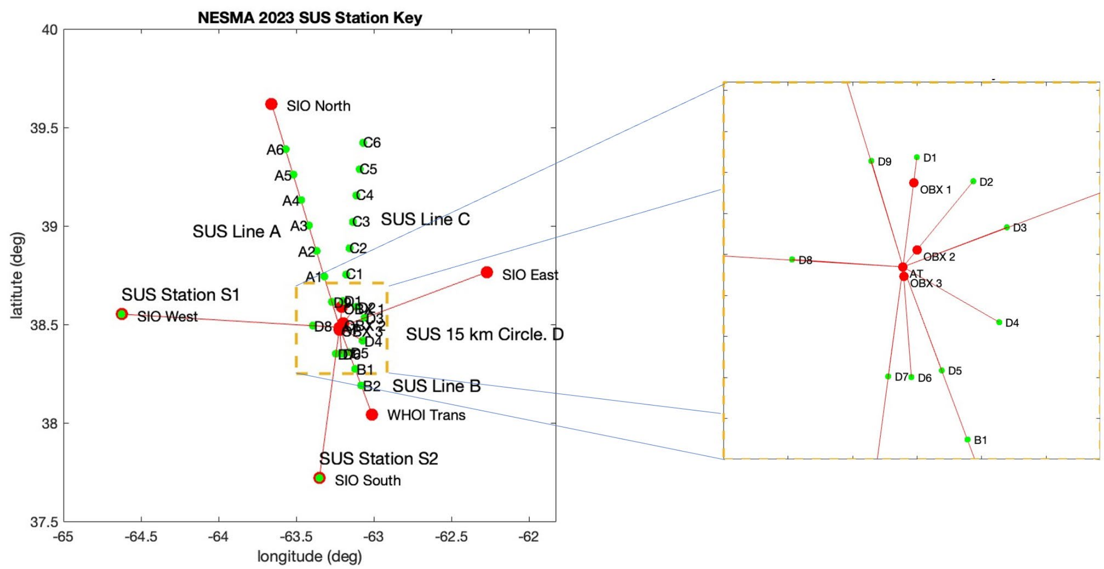

Figure 4. A more detailed view of SUS and OBX deployment around the Atlantis II Seamount (right) detailed view of SUS Circle D with OBX locations.

A total of 120 SUS charges of 1.1 oz weight and designed to detonate at 800 ft (≈243 m) are planned to be distributed at each of the 9 D-locations, shown on the right-side of Figure 4 above. The SUS (Signal, Underwater Sound) explosive charges will be one of the main sound sources for the NESMA experiment, more importantly the focus for this thesis modeling. An image of a SUS charge is shown below in Figure 5.

Figure 5. Image of a SUS explosive charge. (DOSITS, 2024)

The modeling performed uses the receiver locations of the Ocean Botom Recorders (OBXs) deployed by the University of Rhode Island. These OBXs (seen below in Figure 6) are commercially available vector sensors equipped with a hydrophone, for recording pressure, and 3-axis geophones, for recording particle velocity in three directions: inline, crossline, and vertical. (GEOSPACE Technologies, 2023). Three OBXs were deployed on and around the top of the seamount, and their respective locations are seen on the right-side of Figure 4 above. For the purposes of the modeling for this thesis, the focus was narrowed onto the source to receiver line of location D6 to OBX3.

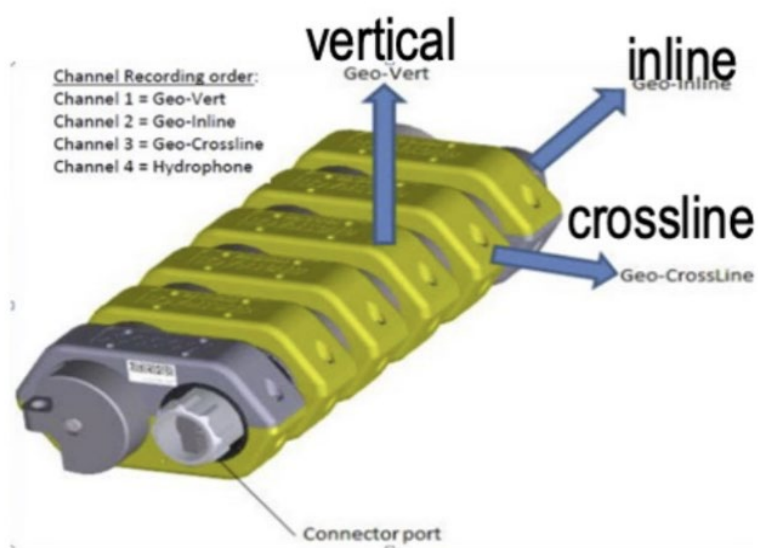

Figure 6. Diagram of Ocean Bottom Recorder (OBX).

Chapter 2. Geologic & Oceanographic Environment

Sub-Bottom Structure

The ocean floor on and around the New England Seamounts contains a sub-bottom structure consisting of a top layer of fine-grained sediments, a layer of limestone beneath the sediment, and a bottom layer of basalt. Below in Figure 7 is a set of sub-bottom profiling data of this sub-bottom structure, obtained from a preliminary AUV survey done in the area.

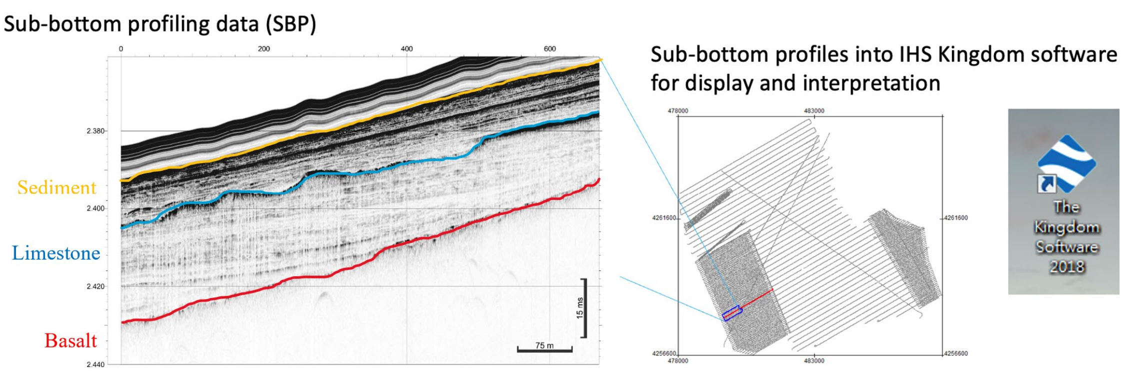

Figure 7. Seamount sub-bottom structure around the Atlantis II seamount obtained from AUV survey. (Personal Communication, Tzu-Ting Chen)

Figure 8 below shows the sediment layer thickness on and around the seamount

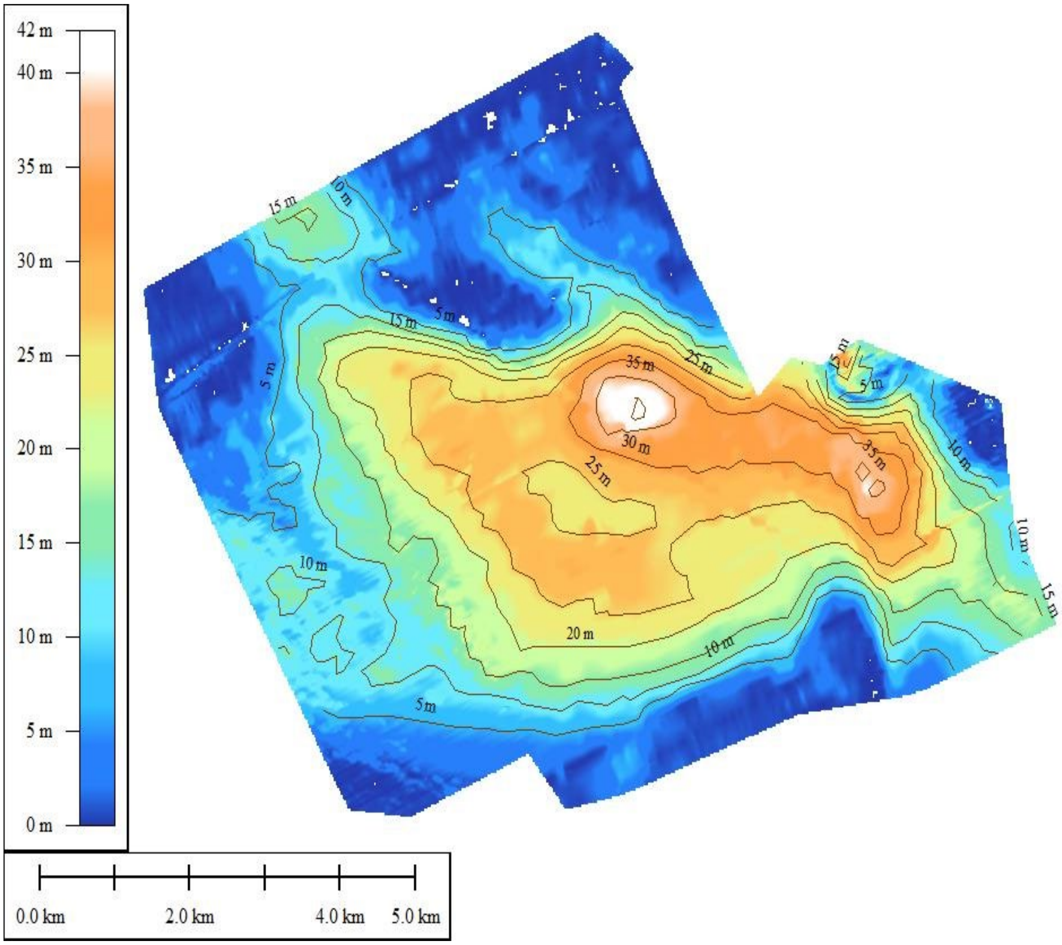

Figure 8. Sediment layer thickness on and around the Atlantis II seamount. (Personal Communication, Tzu-Ting Chen)

It is observed that there is a concentration of sediment on top of the seamount, and the thickness of that layer lessens on the slopes around the seamount. Below in Figure 9 shows the limestone layer thickness around the same area.

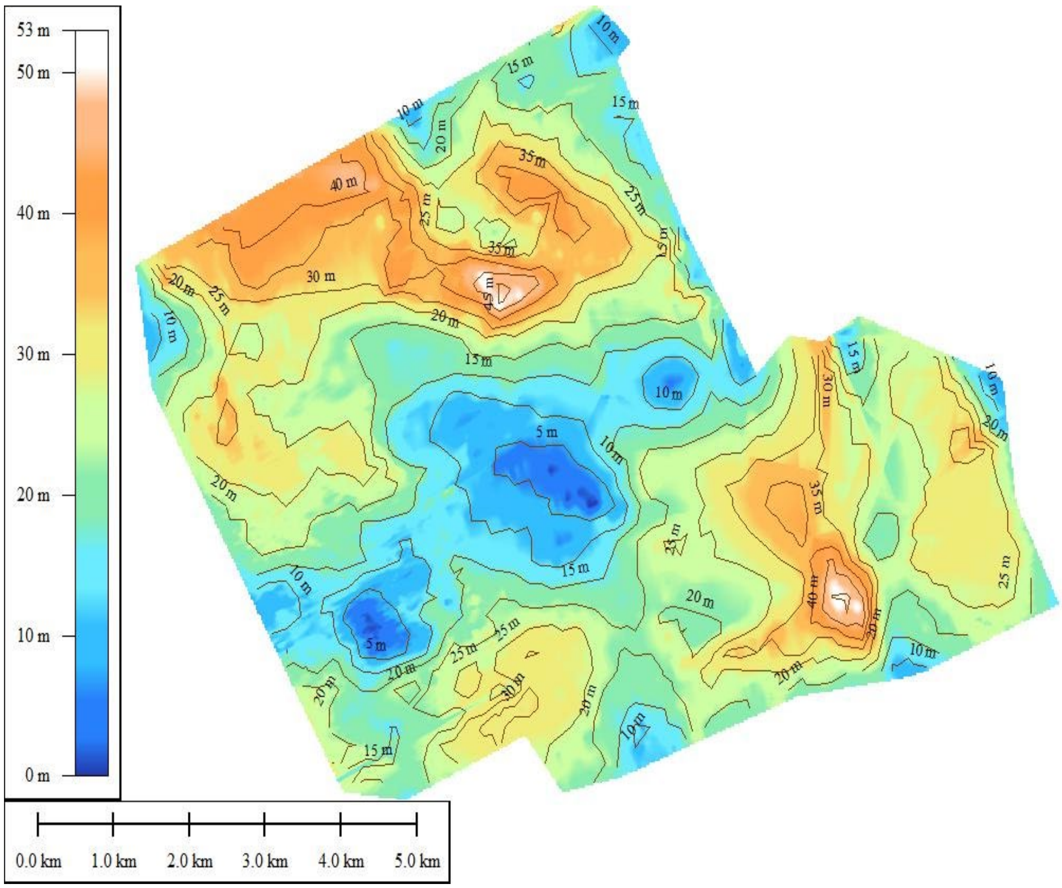

Figure 9. Limestone layer thickness on and around the Atlantis II seamount. (Personal Communication, Tzu-Ting Chen)

It is observed that there are some heavy concentrations of limestone around the base of the seamounts, with much smaller levels of limestone on top of the seamount

Along with this sub-bottom structure, the area contains very complex bathymetry, with lots of jagged rocks seen during some preliminary surveys performed in the seamount area. These jagged rocks combined with the up-slope sound propagation are expected to cause scattering in the area.

Gulf Stream

The Gulf Stream's fast currents and temperature variation in, above, and below it presents an interesting dilemma for researchers performing experiments in the area, and therefore many complexities that need to be considered in their modeling efforts. The Gulf Stream mixes cold water from the North Atlantic with warm, tropical water in the sargasso sea through its strong currents that travel from the tip of Florida to the middle of the Atlantic Ocean. Figure 10 below contains two images of the Gulf Stream, the left representing the sea surface temperature and the right representing the currents in the area.

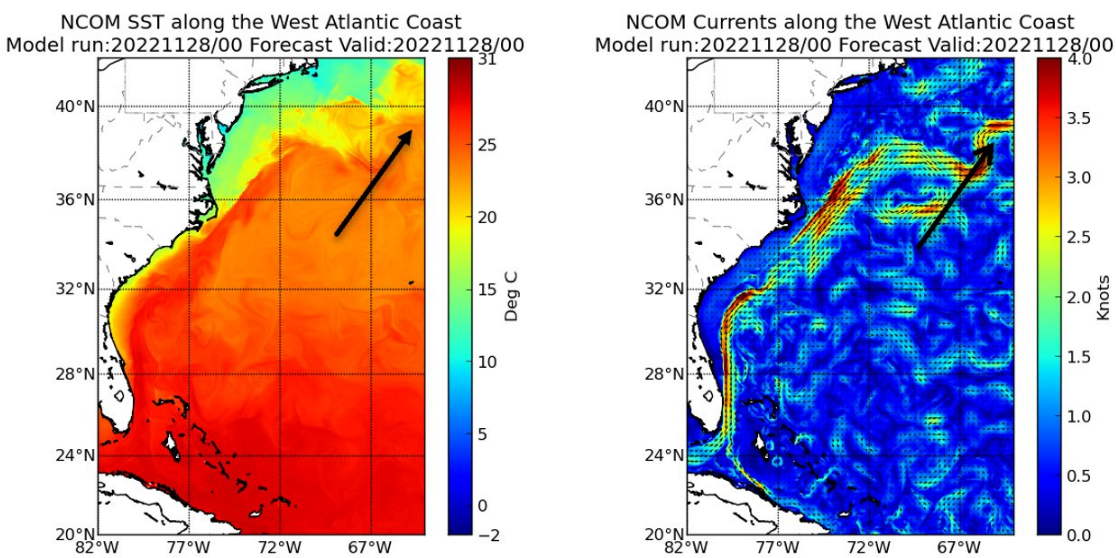

Figure 10. Gulf Stream SST and corresponding currents off the eastern coast of the United States, arrows indicating the location of the New England Seamount Chain. (Tustison N., 2023)

When modeling an ocean environment, the bathymetry and sound speed profiles in the desired environment are crucial to producing an accurate model. Along with the scattering caused by intricate bathymetry, sound speed plays a huge role in how sound will propagate in a certain area. Sound waves expand outward from a source and will continue to propagate outward until this energy is dissipated throughout the ocean, due to effects like absorption into the water column and geometric spreading. Sound will also be refracted throughout its propagation from changing factors like temperature and salinity, both of which influence the sound speed in the water column. In the ocean sound speed varies with depth, so refraction in the vertical direction will occur from sound bending from higher sound speeds to lower sound speeds. The changes in sound speed need to be represented in modeling efforts in order to properly capture the effects on acoustic propagation. Due to the fact that the gulf stream not only mixes warm and cold water, bringing in varying sound speed profiles in water column, as sound will travel slightly faster in warmer waters. The Gulf Stream's location will also fluctuate in the north and south directions, again adding another complexity of the ocean environment being modeled.

Chapter 3. Acoustic Propagation Modeling

BELLHOP Modeling

The first iteration of modeling performed used the BELLHOP ray tracing model (Porter M., 2023) in order to calculate the acoustic paths sound will take in the source to receiver line SUS location D6 to OBX3. This program utilizes a beam tracing model to make these predictions and given the specific source to receiver line that is aiming to be modeled, the model's ability to both produce results on general ray paths as well as specific eigenrays become the main focus. The general ray trace will allow for a visual description of energy both arriving at the proposed receiver location, along with how energy may scatter and dissipate in the water column. Along with the ray trace, the model will be used to calculate all eigenrays along the source-to-receiver line and their respective arrival times. The ray trace modeling performed for this thesis was restricted to a 2D model, so no out-of-plane effects were considered in the model's calculation.

In terms of parameter input for this ray tracing model, the main environmental information fed to the model are the sound speed profile in the water column and the bathymetry of seafloor. The first iteration of runs used a 25-meter resolution bathymetry dataset for the area. Below in Figure 11 displays the bathymetry along the source to receiver in this 2D ocean environment.

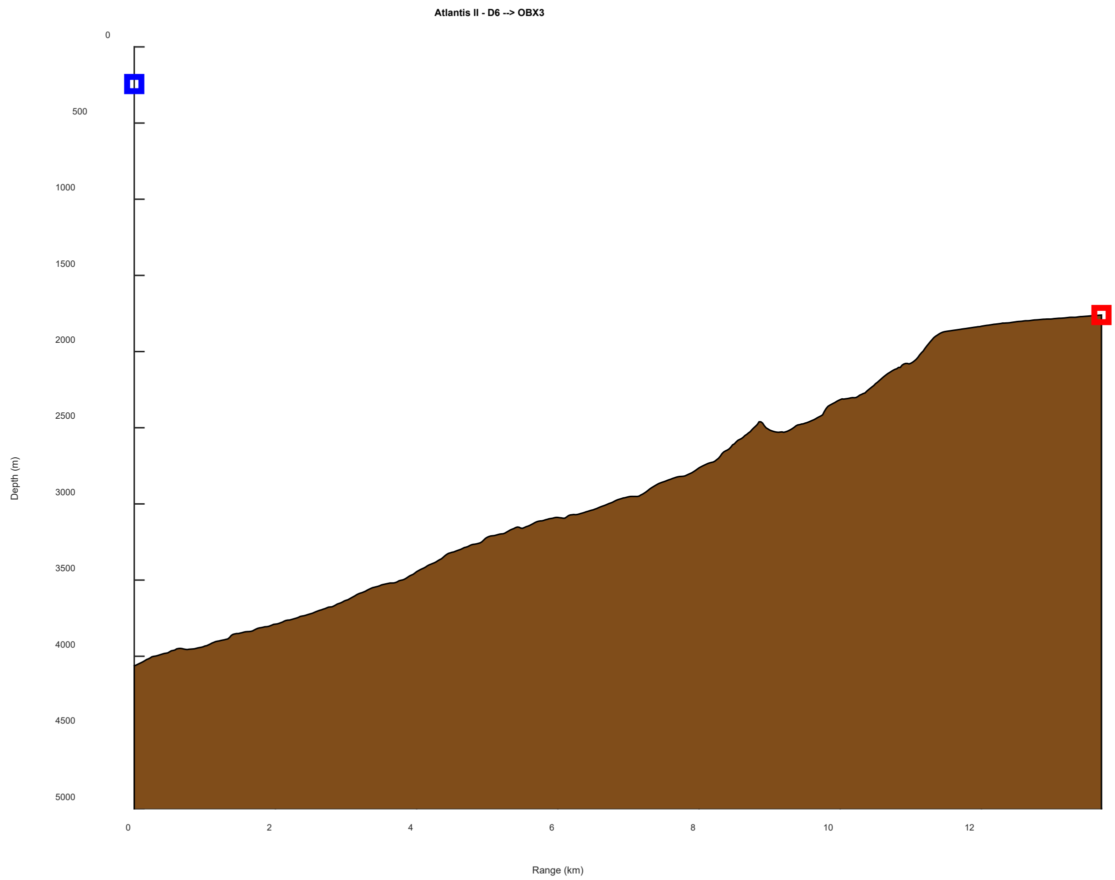

Figure 11. Bathymetry along SUS Location D6 to OBX3. Blue square represents SUS detonation location, red square represents OBX3 location.

This bathymetry grid was compiled through a multitude of data sources and surveys. The primary data source was a 25-meter grid provided by USGS which was compiled through two surveys performed by NOAA and their NOAA OKEANOS EXPLORER, Survey EX1303 from in June of 2013 and Survey EX1404L1 from August of 2014. This grid was vetted to determine any bad values within the dataset, and these were to be removed and filled with simple, linear interpolation.

The second main environmental parameter is the sound speed profile in the water column. As discussed in Chapter 2 of this thesis, there are many complexities in the makeup of this sound speed profile induced from the Gulf Stream, bringing in varying water temperature and in turn varying sound speeds. A prior graduate student, Nathan Tustison, had performed some preliminary modeling for the NESMA experiment, and a large piece of that work included the compilation of temperature, salinity, and depth data from the World Ocean Database for the calculation of sound speed profiles in the seamount area. These varying profiles were then averaged to create two sound speed profiles, a "warm side" SSP and "cold side" SSP, for the purpose of attempting to represent two different ocean environments the changing location of the Gulf stream can create. (Tustison N., 2023)

Below in Figure 12 are graphs depicting the salinity and temperature compiled for calculating the sound speed profiles.

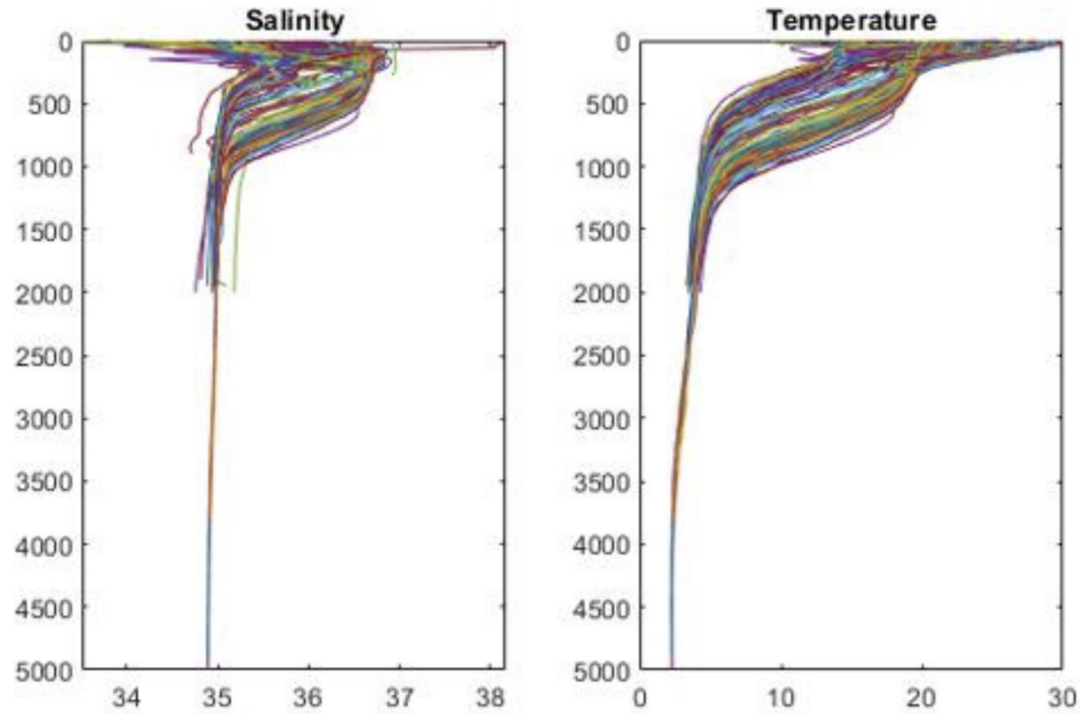

Figure 12. Temperature and salinity data from World Ocean Database in the NESMA experiment area.

Below in Figure 13 are two graphs from this paper showing the cold, warm, and average sound speed profiles calculated, as well as the calculated datasets from which they were derived.

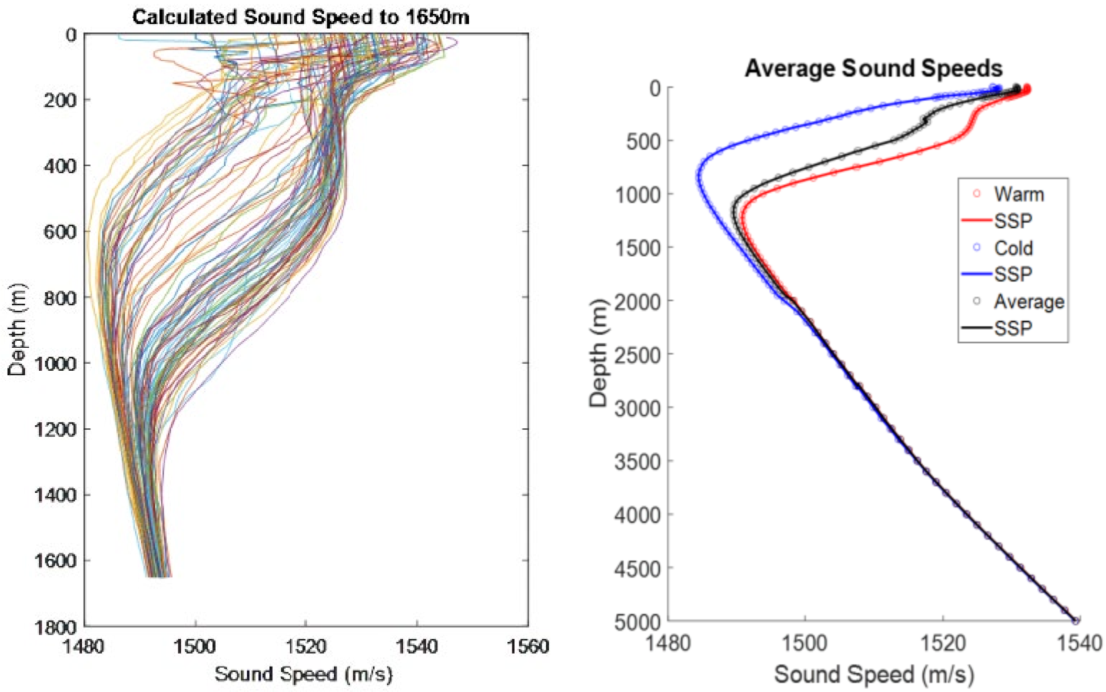

Figure 13. (left) Calculated sound speed profiles for Atlantis II Seamounts (right) Average sound speed profiles for the "warm side" and "cold side" scenarios, as well as an overall average sound speed profile. (Tustison N., 2023)

Broadband PE Modeling

Parabolic equation modeling is a widely used approach for modeling acoustic propagation in the ocean and is known to produce very accurate representations of this sound propagation. The combination of using a robust ray tracing model with BELLHOP with an accurate PE model can be very powerful in understanding the acoustic propagation in an ocean environment. For this thesis the MMPE model will be used, a model produced by Fred Tappert and Kevin Smith, which is an expansion on the single frequency UMPE model to have broadband capabilities (Tappert, F., Smith, K.B., 2023).

Due to certain restrictions in the strength of the model, the resolution of the bathymetry and sound speed profiles had to be lowered to successfully produce results. Given that the focus of this thesis is on low-frequency sound propagation, a bandwidth of 100 Hz ranging from 100 Hz to 200 Hz will be modeled and analyzed. Another main reason this model was chosen over other models is its ability to model a broadband source. Most PE models are designed for a single frequency, but since the SUS explosives used in the NESMA experiment are broadband sources, it has been concluded that the MMPE will produce the most accurate representation of this acoustic propagation. The MMPE also requires a set of bottom properties to be selected in the environmental files. As discussed prior, there has been some level of AUV surveys of the sub-bottom structure on and around the seamount, however there has yet to be any firm and substantial coverage models of this sub-bottom sediment stratification. Until more parameters are established for this sub-bottom, a homogenous bottom model will be used for the PE modeling. The model will use properties of a silty-sand bottom, with a sound speed of 1650 m/s, a density of 1.83 kg/cm^3, a compressional attenuation of 0.0619 dB/m/kHz.

Given that the data analysis portion of this thesis will be focusing on pressure data collected by the hydrophone on the OBX, the acoustic pressure will be selected from the model's output. For the way that the model is currently designed, the output that it provides is the complex envelope, which needs to be converted to the complex pressure using the equation below.

$$x(t) = Re(\hat{x}(t)e^{-j2\pi f_c t})$$

where $x(t)$ is complex pressure, $\hat{x}(t)$ is the complex envelope function, f_c is the center frequency, and t is the time series (Ziomek L. J. 1995).

Chapter 4. Modeling Results

The BELLHOP model was run for the two varying sound speed profiles mentioned prior, and the ray trace results and eigenray arrival plots can be seen below in Figure 14 and Figure 15.

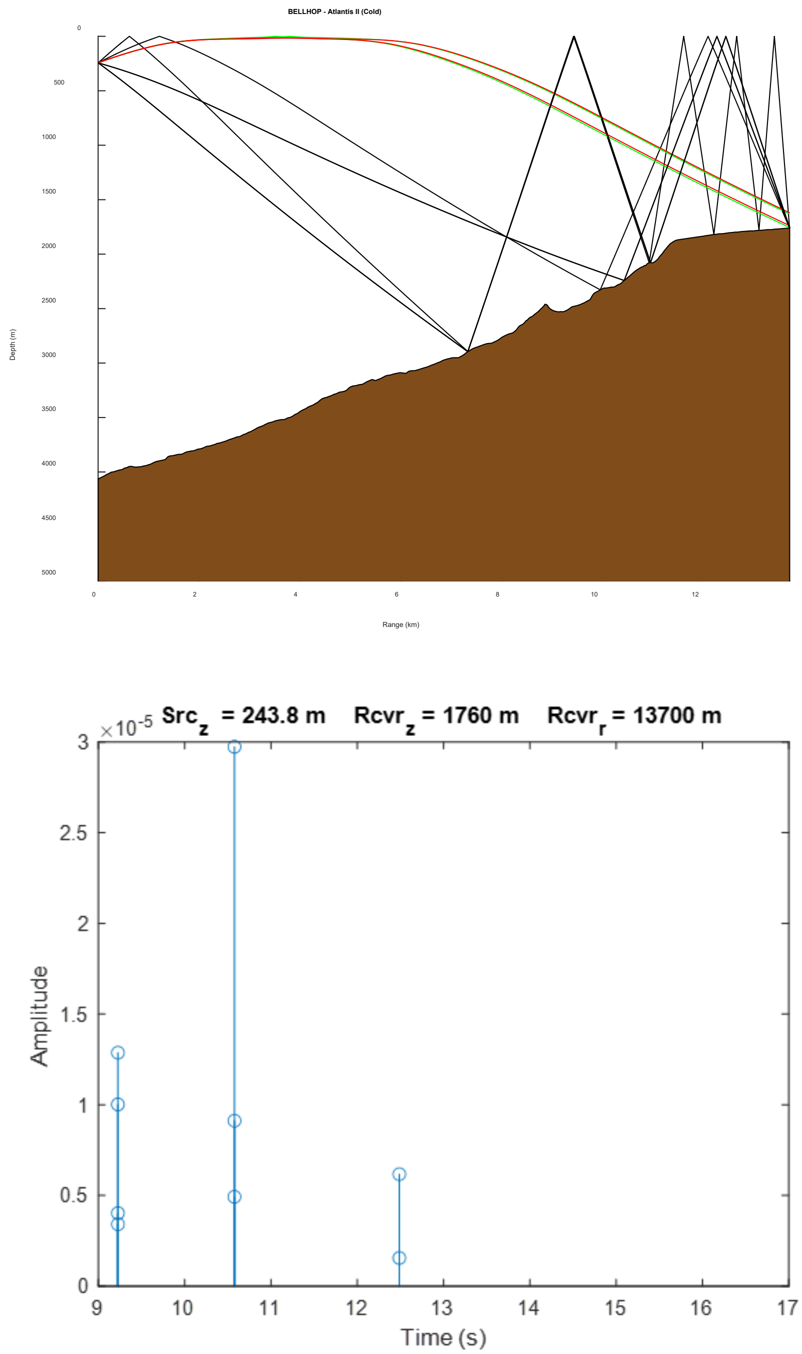

Figure 14. (top) Ray trace for the “cold side” sound speed profile. (bottom) Eigenray arrival plot for “cold side” sound speed profile, with time axis defined as travel time.

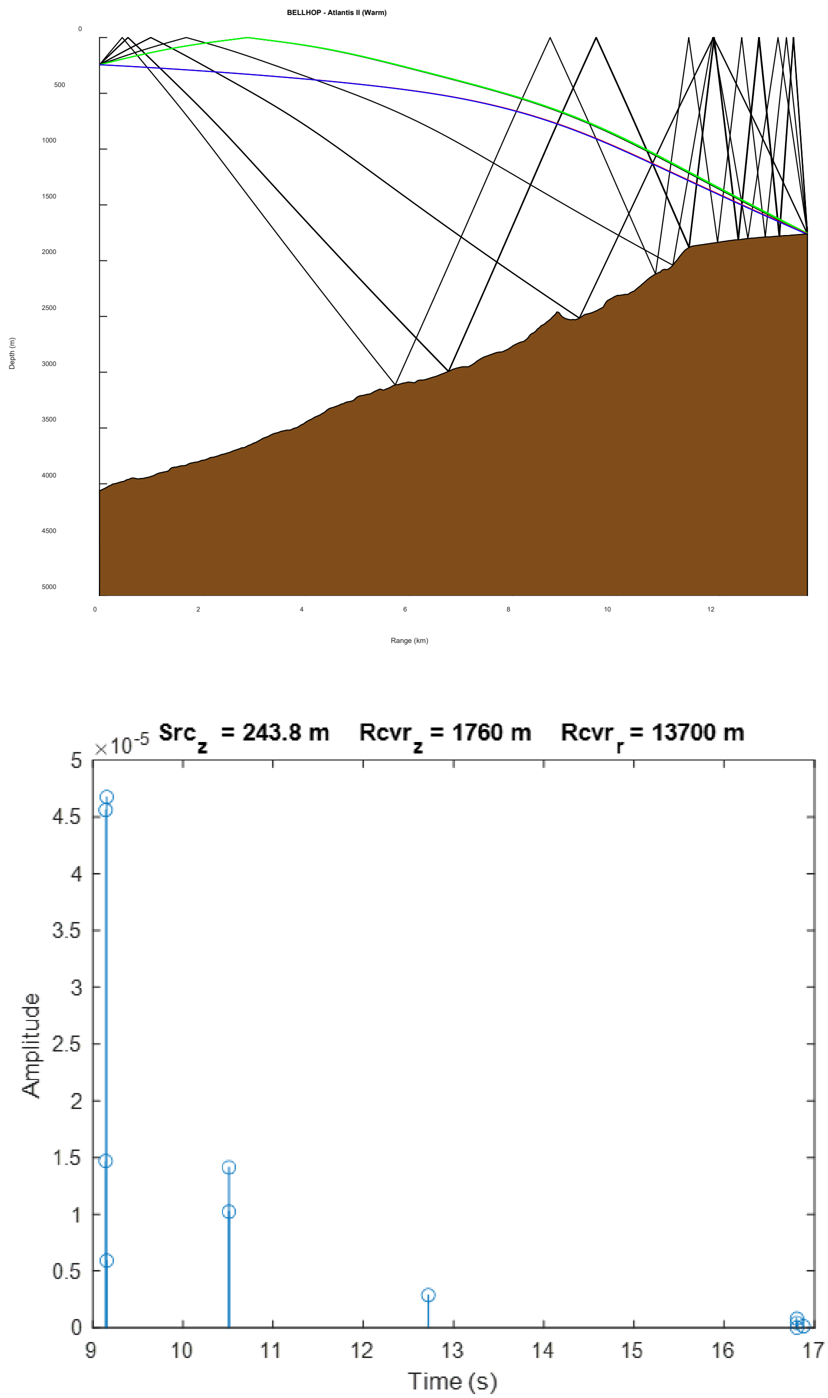

Figure 15. (top) Ray trace for the "warm side" sound speed profile. (bottom) Eigenray arrival plot for "warm side" sound speed profile, with time axis defined as travel time.

As seen in the figures above, there appears to be three defined sets of arrivals for both cases, with a late fourth arrival seen with the warm sound speed profile. The first arrival shows the direct arrival and surface bounce eigenray path, the second arrival shows eigenray paths with some bottom to surface interaction, and the third arrival shows eigenray paths with multiple bottom to surface interactions. The arrivals within the warm sound speed scenario appear to have slightly faster arrival times than the cold sound speed scenario, a result that is expected due to the faster sound speeds associated with the "warm side." The warm sound speed profile appears to create a stronger first arrival, whereas the cold sound speed profile creates a stronger second arrival. This variation is a confirmation of the expected differences between the varying sound speeds in and around the Gulf Stream.

The MMPE was then run for both ocean environments used in the BELLHOP model runs, and each of their respective eigenray arrival plots are shown directly below each complex pressure time series obtained from the MMPE model runs in Figure 16 and Figure 17 below.

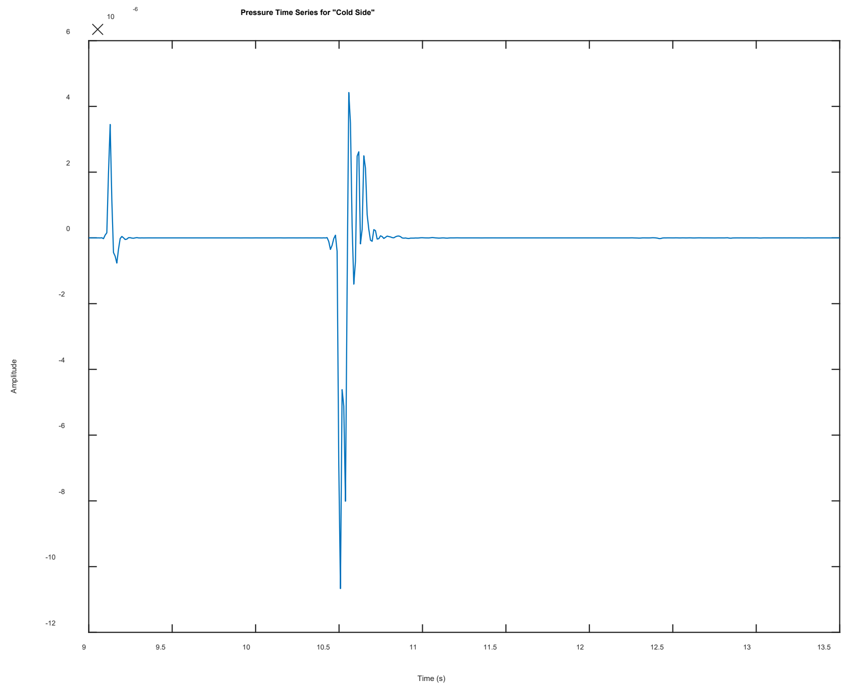

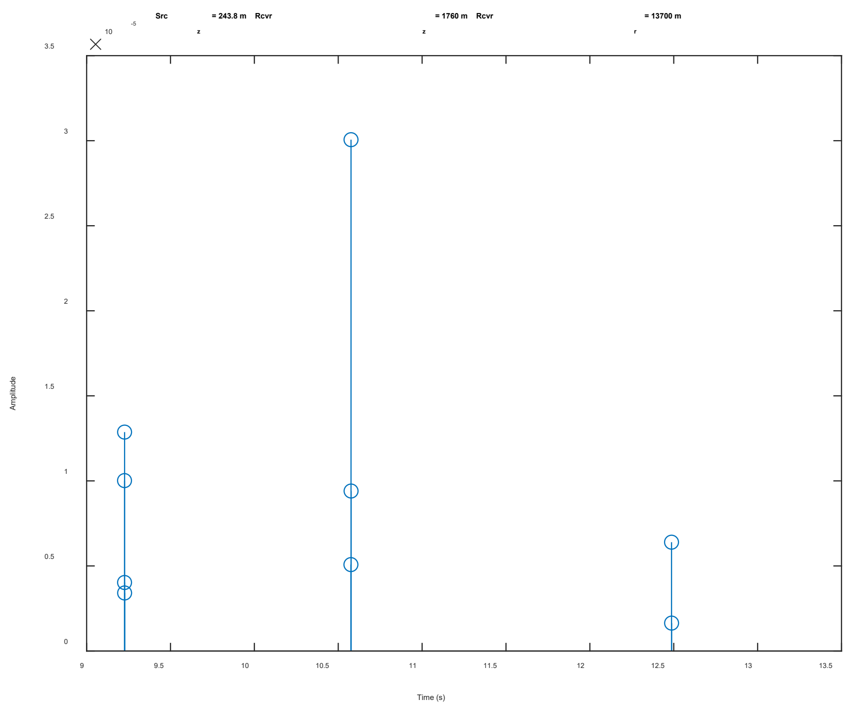

Figure 16. (top) Pressure time series for the “cold side” sound speed profile with (bottom) respective eigenray arrival plot. Both time axes are defined as travel time.

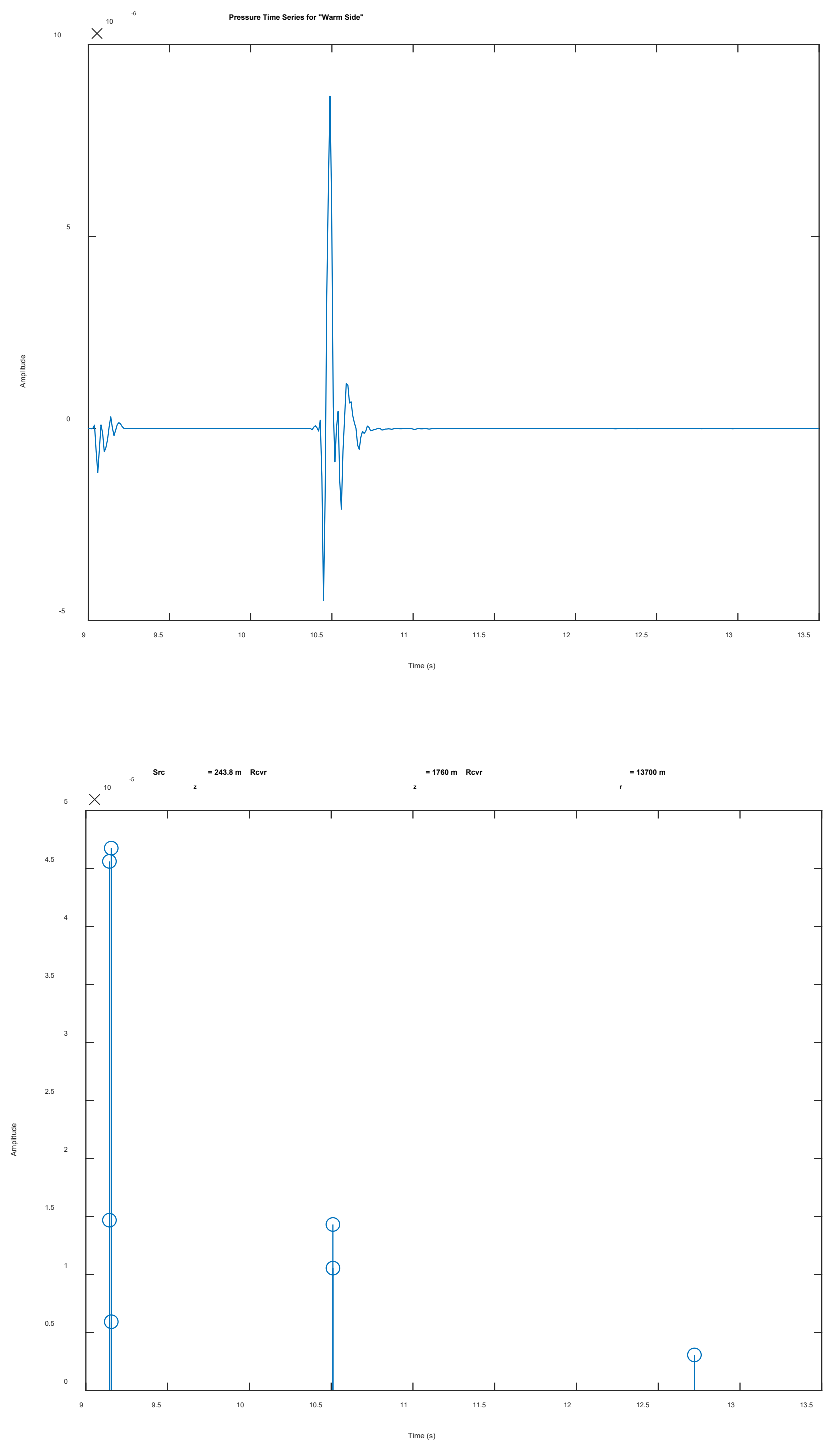

Figure 17. (top) Pressure time series for the “warm side” sound speed profile with (bottom) respective eigenray arrival plot. Both time axes are defined as travel time.

As seen in the figures above in both ocean environments, the arrival times of the three main sets of ray arrivals align in both the MMPE model and BELLHOP model, showing agreement between the two models. Below are two spectrograms showing the sound pressure level distribution for both the “cold side” and the “warm side.”

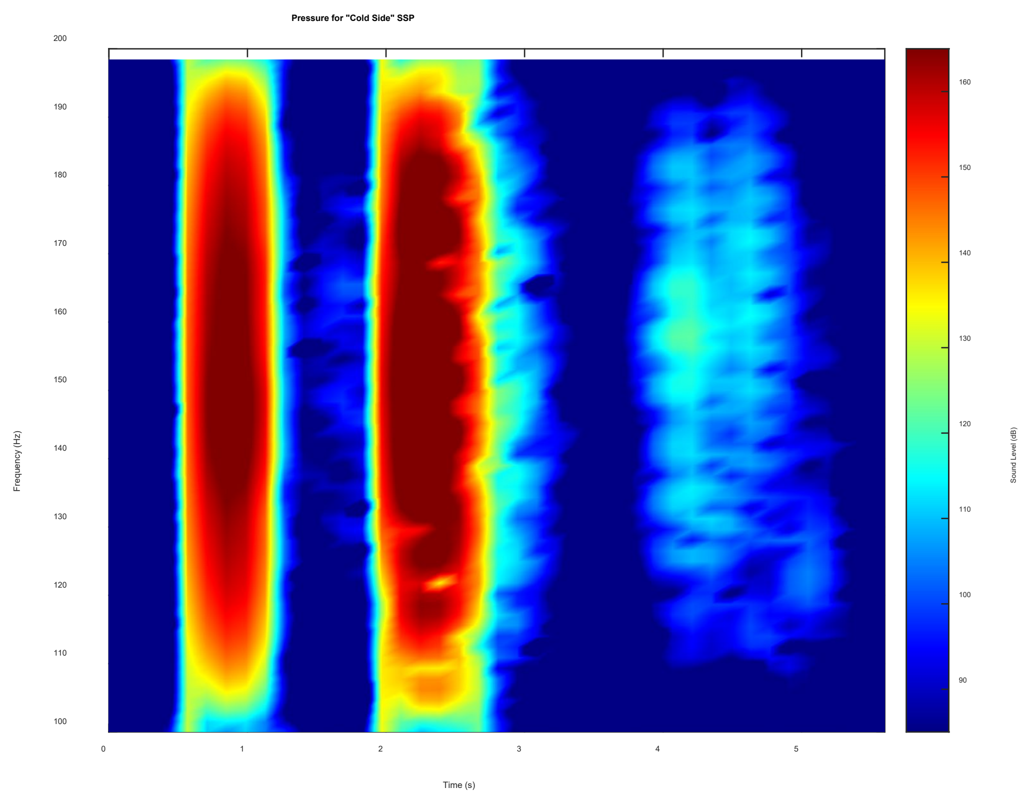

Figure 18. Spectrogram of sound pressure level for “cold side” sound speed profile. Time axis is set to arbitrary time.

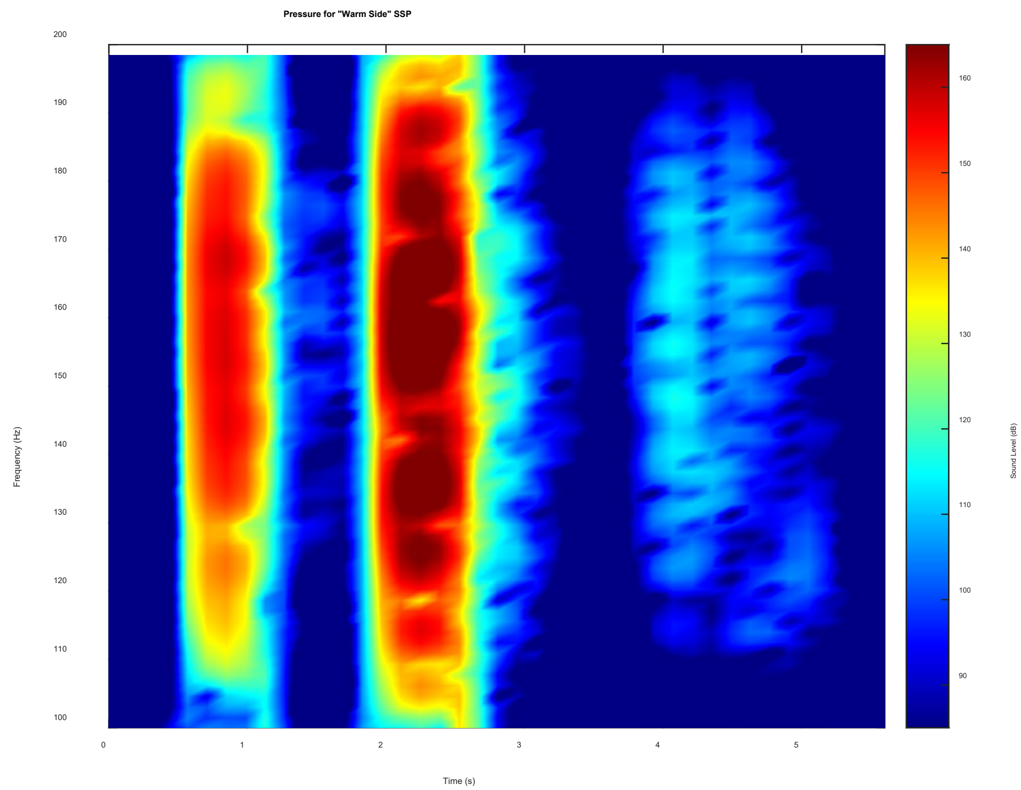

Figure 19. Spectrogram of sound pressure level for “warm side” sound speed profile. Time axis is set to arbitrary time.

It is observed that that the distribution of energy between the first two sets of arrivals varies between the two different sound speed profiles, as also shown in the BELLHOP model results.

Chapter 5. Data Analysis

During the NESMA experiment in 2023, there were a total of 21 SUS explosives dropped at the SUS Location D6 over the course of an hour, and 20 of these explosives were successfully recorded by the OBX. There was one of the explosives reported to be a dud, which infers that the explosive never detonated after its release from the ship. Below in Figure 20 is a spectrogram of the hydrophone data recorded for one of these SUS explosives.

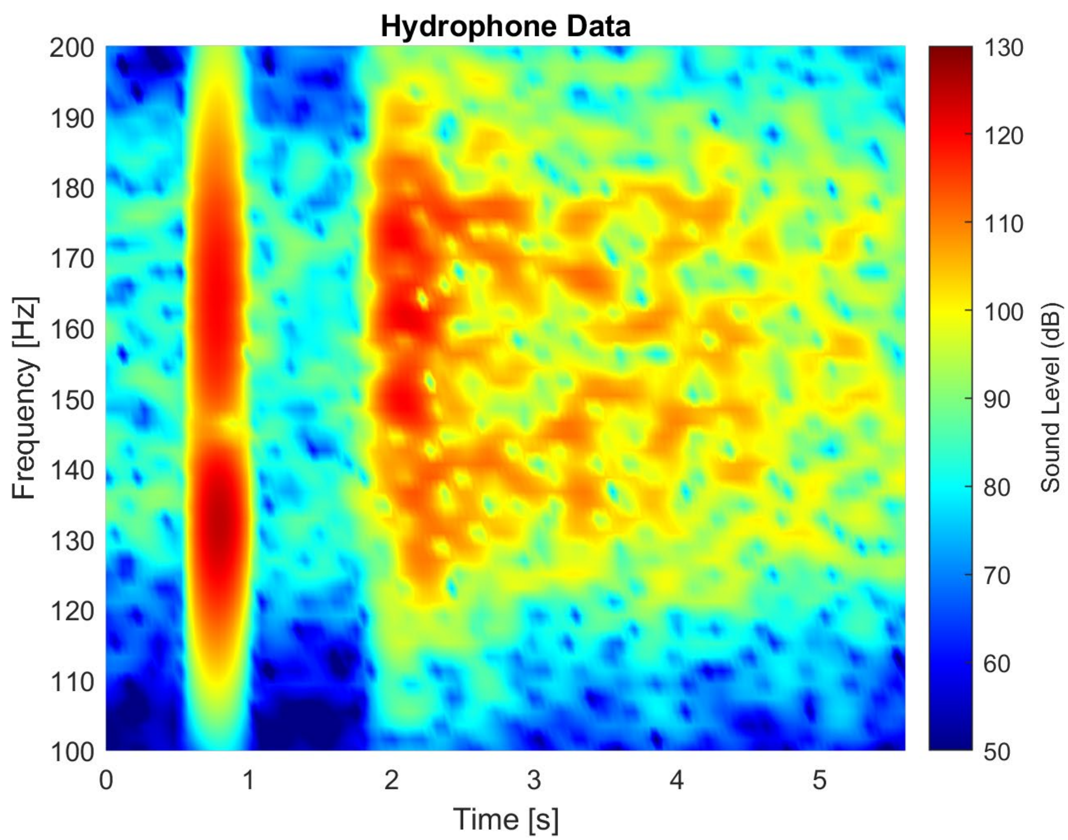

Figure 20. Hydrophone data of SUS explosive at SUS Location D6. Time axis is set to arbitrary time.

Below in Figure 21 is again the hydrophone data of a SUS explosive shown above, with both spectrograms for the varying ocean environments run through the MMPE model.

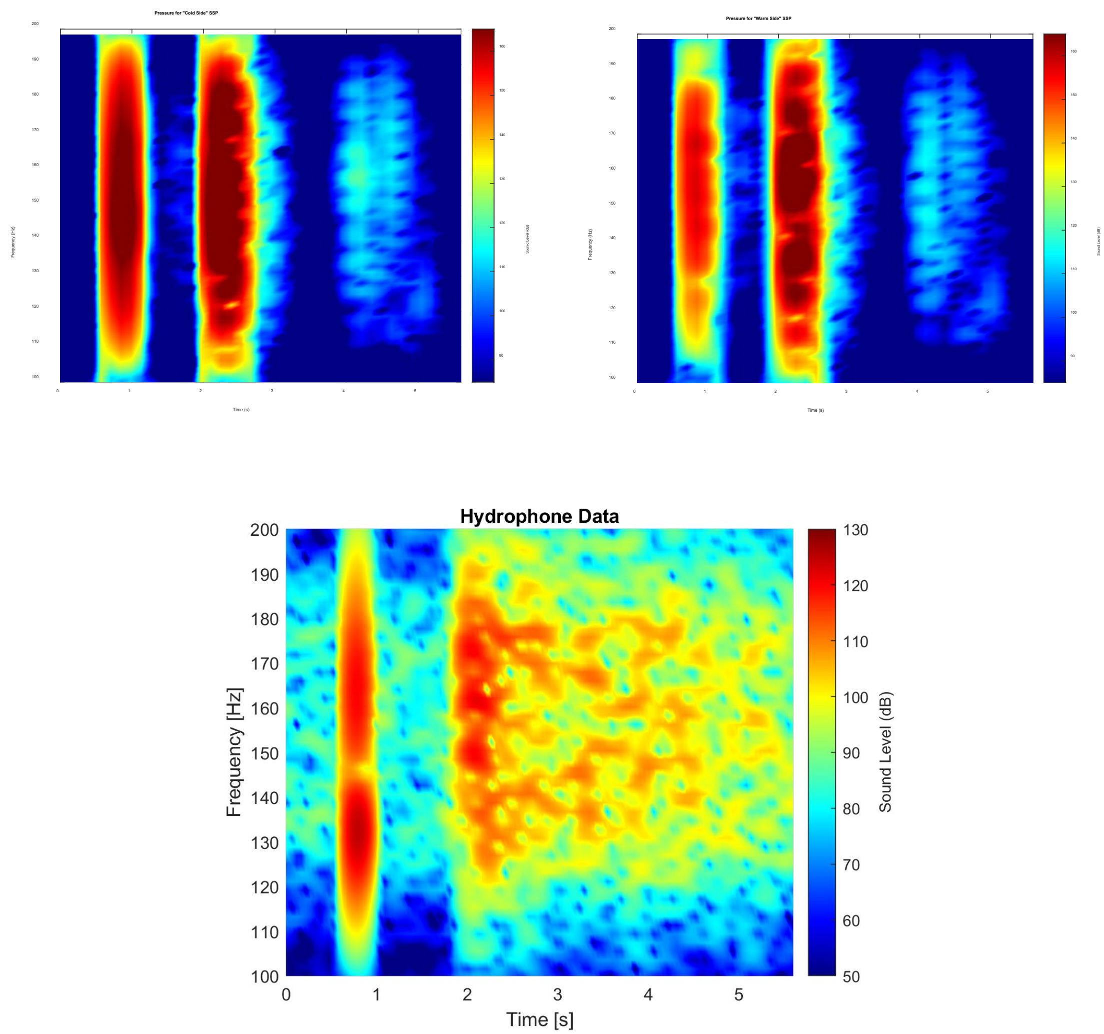

Figure 21. (top) Complex Pressure for both (left) “cold side” and (right) “warm side” sound speed profiles. (bottom) Hydrophone data for SUS explosive at SUS Location D6. Time axis is set to arbitrary time.

Now comparing the MMPE model results to the collected data from the experiment, it is seen that the first two sets of arrivals both arrive with a very similar arrival time difference between the model and real data. The time axes for each spectrogram are zeroed out and assumed to be arbitrary. The third arrival does not appear to be defined in the real data, which may be due to a variety of factors. There is a lot more observed distribution of energy throughout the real data, whereas it appears to be much more concentrated in the model output. The MMPE is a 2D model that does not consider any out of plane effects, so those effects could be a factor in the greater energy distribution, whether it be out of plane energy arriving at the OBX or energy being seen in the model that may have deflected out of plane. The bathymetry input for the MMPE is also not nearly as high of a resolution to fully encapsulate all the complexities on the ocean floor, as it had been previously discussed there has been many jagged rocks observed on and around the seamount environment. This lack of energy distribution in the model may be in part due to the lack of a complete representation of the ocean floor in its environment files.

Chapter 6. Modeling Results for NESMA 2024 Experiment

This modeling can now be applied to perform some preliminary modeling for the upcoming NESMA experiment taking place in July 2024. One of the main focuses of this experiment is collecting some acoustic data around the caldera, a tunnel-like feature located southeast of the Atlantis II seamount. The PE modeling scenario performed will use OBX2 as its receiver and a SUS location as its source, 13.7 km away down the caldera. Below is a Google Earth snapshot of both source to receiver lines, the original SUS Location D6 to OBX3 for NESMA 2023, and this SUS model location to OBX2 for NESMA 2024.

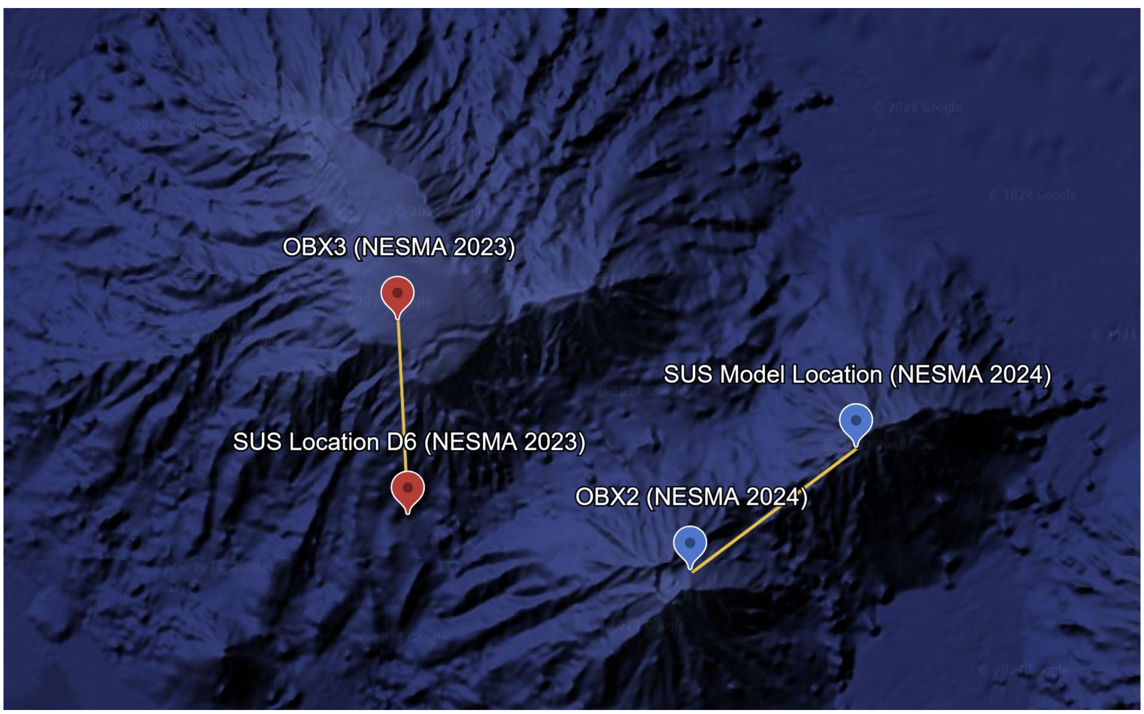

Figure 22. Source to receiver lines for modeling scenarios for NESMA 2023 (red markers) and NESMA 2024 (blue markers)

The bathymetry for this SUS to OBX2 source to receiver line can be seen below in Figure 23.

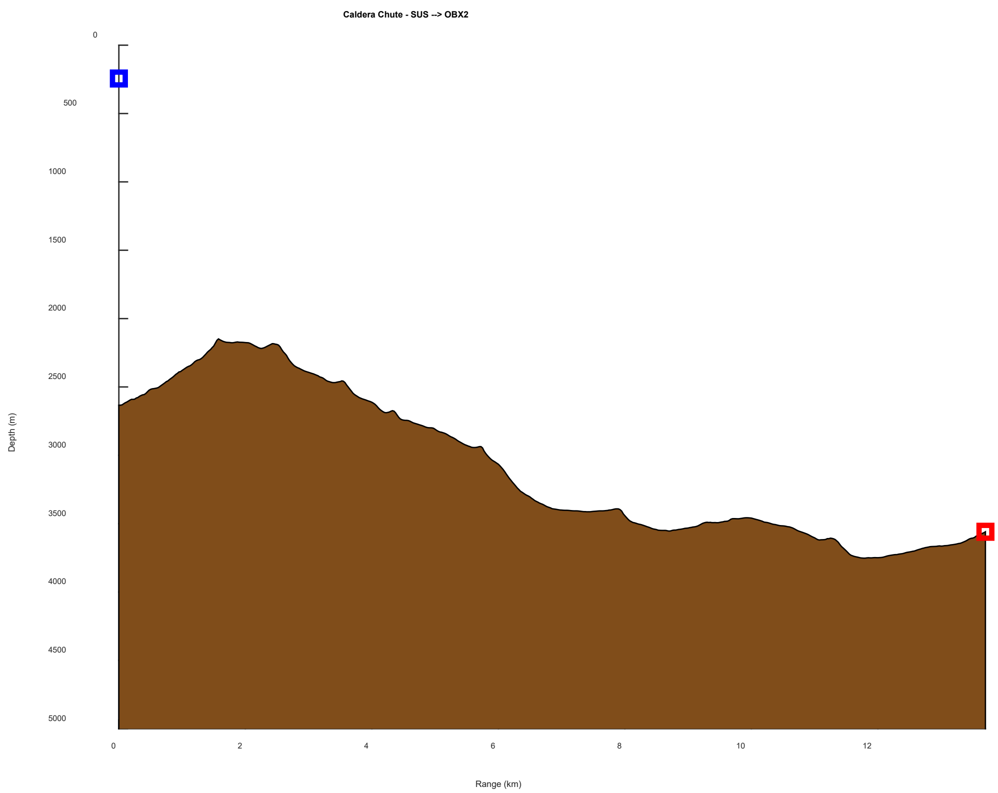

Figure 23. Bathymetry along SUS Location D6 to OBX3. Blue square represents SUS detonation location, red square represents OBX3 location.

Figure 24 below shows the eigenray arrival plot for the “cold side” scenario.

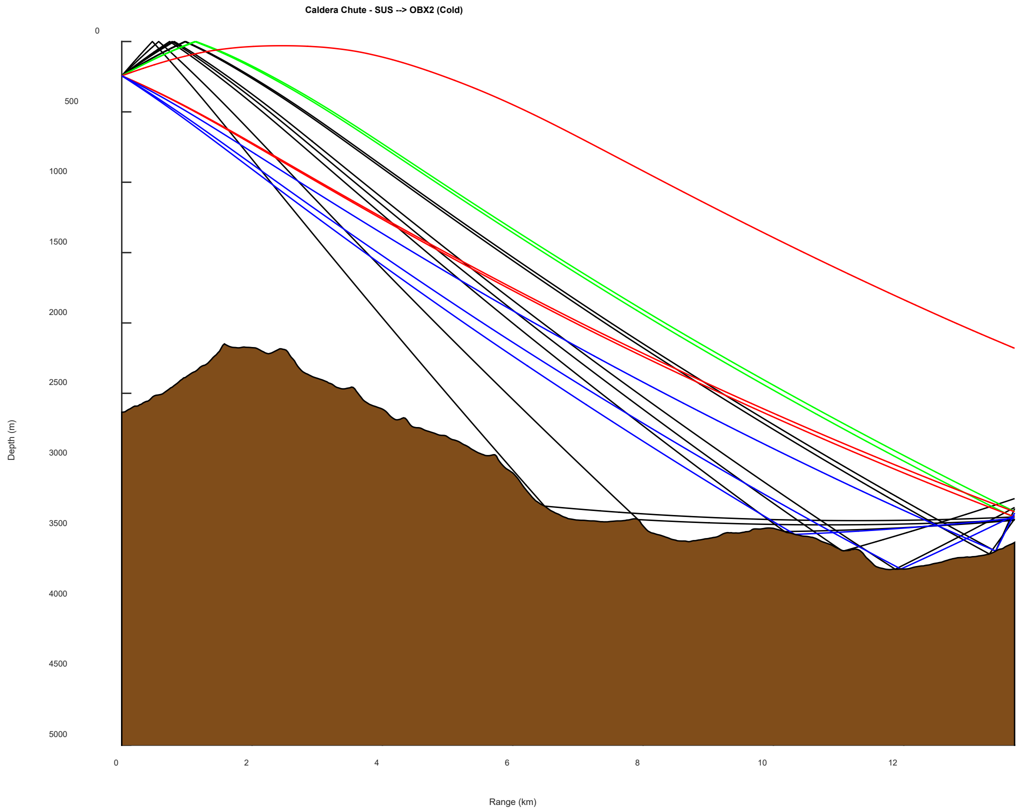

Figure 24. Ray trace for the “cold side” sound speed profile showing eigenray arrivals.

Figure 25 below shows the eigenray arrival plot and the pressure time series for the “cold side” scenario.

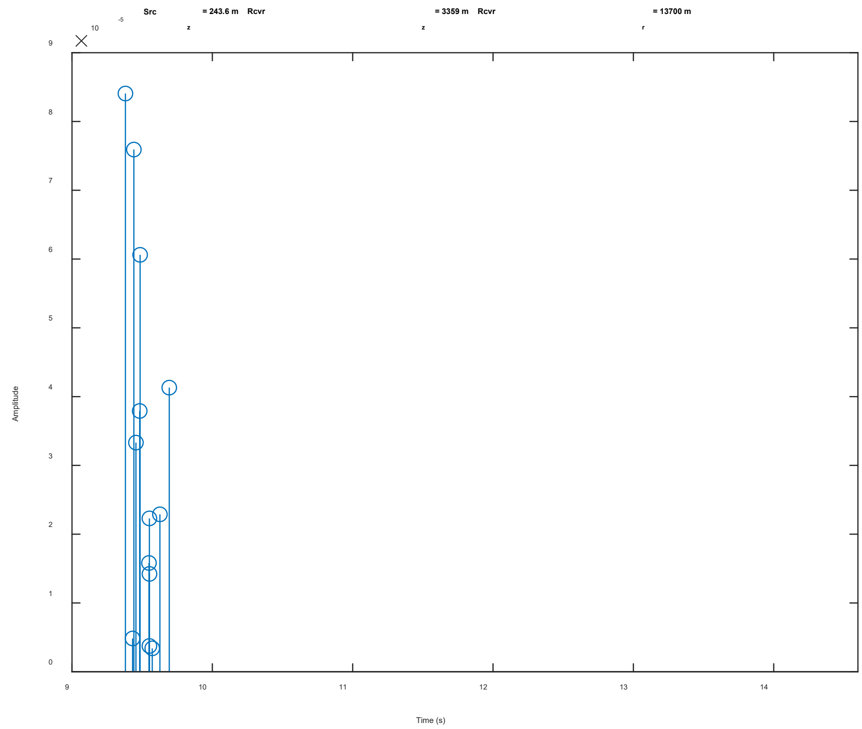

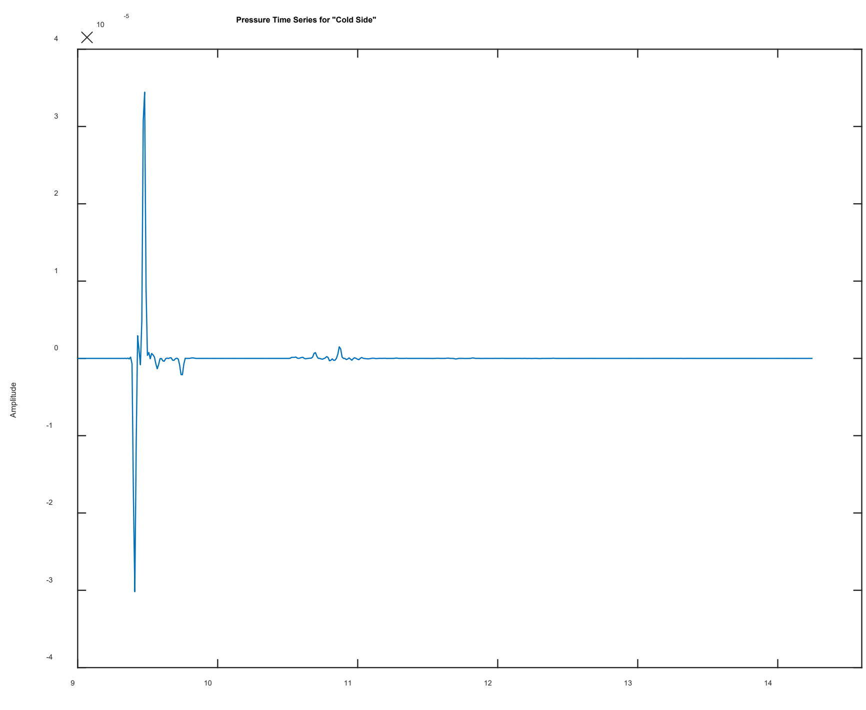

Figure 25. (top) Eigenray arrival plot for “cold side” sound speed profile (bottom) Pressure time series for the “cold side” sound speed profile. Time axes defined as travel time.

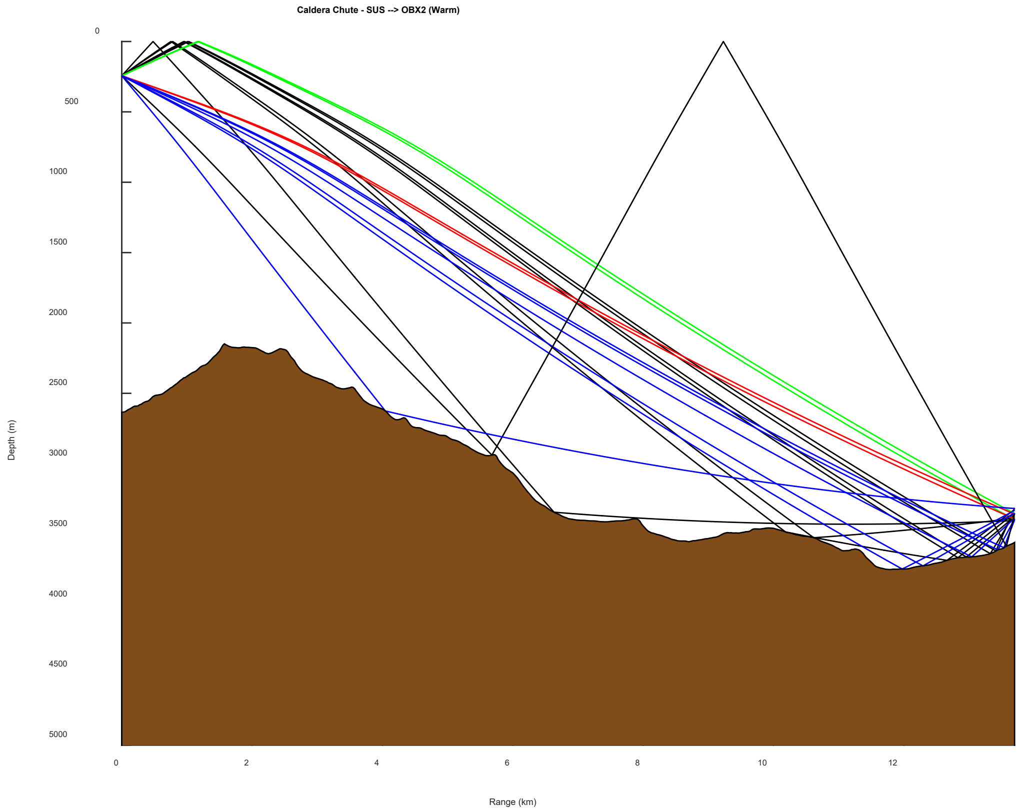

Figure 26. Ray trace for the “cold side” sound speed profile showing eigenray arrivals.

Figure 27 below shows the eigenray arrival plot and the pressure time series for the “warm side” scenario.

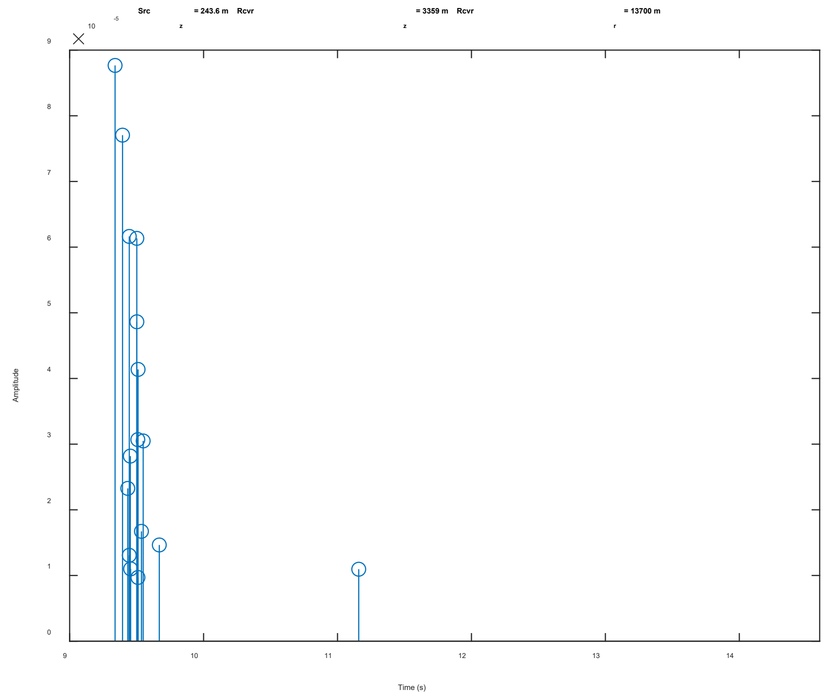

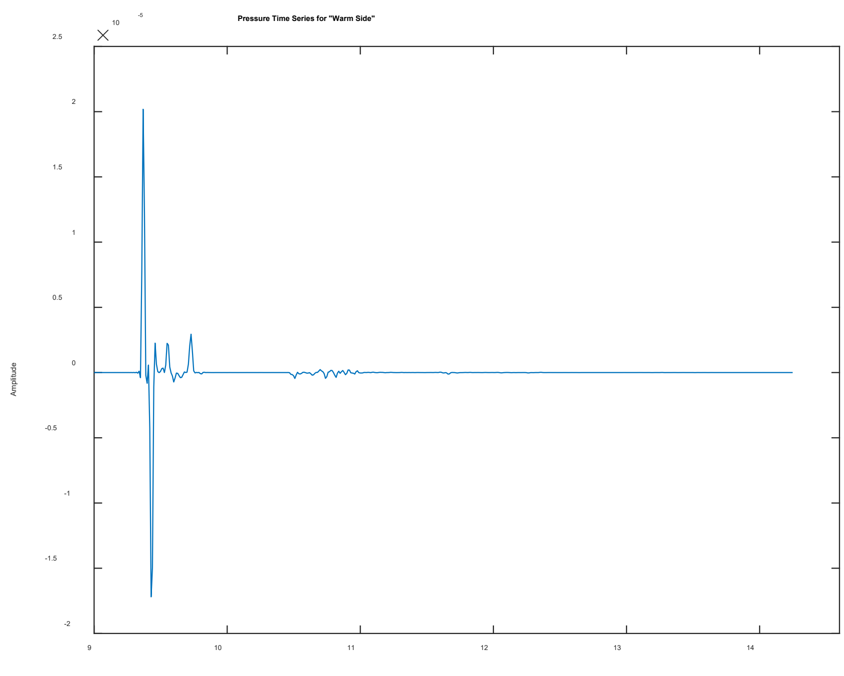

Figure 27. (top) Eigenray arrival plot for "warm side" sound speed profile (bottom) Pressure time series for the "warm side" sound speed profile. Time axes defined as travel time.

Figure 28 below shows a spectrogram of the sound pressure level distribution for the "cold side."

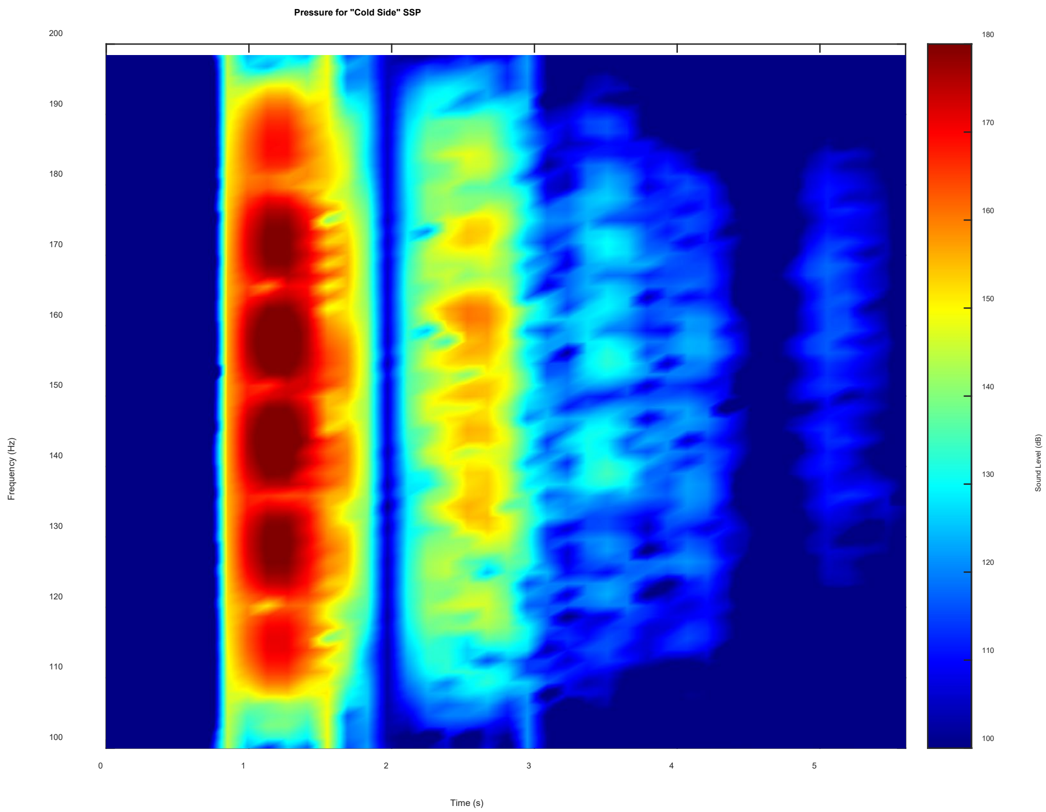

Figure 28. Spectrogram of sound pressure level for "cold side" sound speed profile. Time axis is set to arbitrary time.

Figure 29 below shows a spectrogram of the sound pressure level distribution for the "warm side."

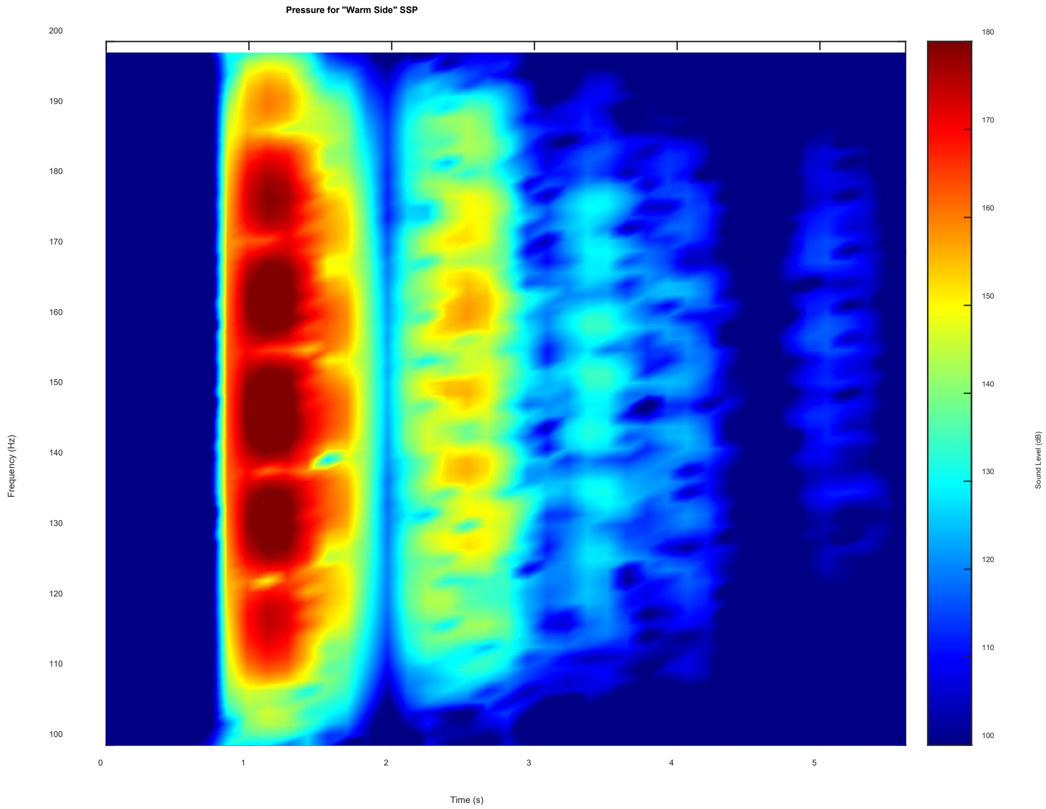

Figure 29. Spectrogram of sound pressure level for “warm side” sound speed profile. Time axis is set to arbitrary time.

The modeling results for both the “warm side” and “cold side” show multiple sets of arrivals, some of which may be interacting with the surface, bottom, or both. Further comparison to collected data from the upcoming experiment will allow for a better understanding of the modeling results.

Chapter 7. Conclusions and Recommendations

The two modelling programs, BELLHOP and MMPE, have been shown to be useful in the modeling of acoustic propagation, both before and after proposed experiments. These models shined light on effects from changing sound speeds and varying bathymetry within different ocean environments. These modelling techniques can be used prior to an experiment to have some preliminary insight into the acoustic propagation of the ocean environment being researched, along with the strengthening of these models through data analysis performed after the experiment. They are another propagation tool to be used in combination with other models to progress and refine acoustic research performed in the ocean environment.

The modelling techniques used in this thesis can be improved, as there were some restrictions with implementing higher resolution bathymetry and sound speed profiles for the MMPE. Further investigation into the model's capabilities can allow for increased accuracy of the modeling results. Given that the sound speed profiles used were produced from historical data, inputting some measured sound speed profiles during the experiments can help create a more accurate ocean environment at the time of the data collection.

Bibliography

DOSITS. (2024, January 12). Explosive Sound Sources. Retrieved from DOSITS: https://dosits.org/galleries/audio-gallery/anthropogenic-sounds/explosive-sound-sources/

GEOSPACE Technologies. (2024, January 20). Marine exploration OBX-90. Retrieved from Geospace technologies: https://www.geospace.com/products/marine-exploration/obx-90/

OC Research. (2024 , July 1). Oceanography - Naval Postgraduate School. (n.d.). https://nps.edu/web/oceanography/research-areas

Navy, U. (2024, January 12). US Navy Task Force Ocean. Retrieved from Office of Naval Research: https://www.nre.navy.mil/organization/departments/code-32/partnerships/task-force-ocean

Porter, M. (2023, February 8). Acoutics Toolbox. Retrieved from HLS Research: http://oalib.hlsresearch.com/AcousticsToolbox/

Tappert, F., Smith, K.B. (2024, January 5), MMPE. Retrieved from: https://oalib-acoustics.org/models-and-software/parabolic-equation/

Tustison, N. (2023), "MODELING ACOUSTIC PROPAGATION NEAR THE ATLANTIS II SEAMOUNTS" (2023). Open Access Master's Theses. Paper 2385. https://digitalcommons.uri.edu/theses/2385

Ziomek, L. J., Fundamentals of Acoustic Field Theory and Space-Time Signal Processing, CRC Press, 1995.